

## Influence of feed concentration and pH on iron and manganese rejection via nanohybrid polysulfone/Ag-GO ultrafiltration membrane

Norherdawati Kasim<sup>a,b,\*</sup>, Ebrahim Mahmoudi<sup>a</sup>, Abdul Wahab Mohammad<sup>a,c</sup>,  
Siti Rozaimah Sheikh Abdullah<sup>a</sup>

<sup>a</sup>Department of Chemical and Process Engineering, Faculty of Engineering and Built Environment, Universiti Kebangsaan Malaysia, 43600 UKM Bangi, Selangor, Malaysia, Tel. +603-90513400, Fax +603-90513028, email: herdawati@upnm.edu.my (N. Kasim), ebi.dream@gmail.com (E. Mahmoudi), drawm@ukm.edu.my (A.W. Mohammad), rozaimah@ukm.edu.my (S.R.S. Abdullah)

<sup>b</sup>Department of Chemistry, Centre for Defence Foundation Studies, National Defence University of Malaysia, Kem Sg. Besi, 57000 Kuala Lumpur, Malaysia

<sup>c</sup>Research Centre for Sustainable Process Technology (CESPRO), Faculty of Engineering and Built Environment, Universiti Kebangsaan Malaysia, 43600 UKM Bangi, Selangor, Malaysia

Received 13 December 2015; Accepted 26 June 2016

### ABSTRACT

Iron and manganese are elements that exist naturally in water, especially groundwater. The aim of this work is to study the rejection mechanisms of iron and manganese at various feed concentration and investigate the influence of pH on metallic ions rejection using fabricated polysulfone (PSF) incorporated with silver-decorated graphene oxide (Ag-GO) ultrafiltration (UF) membrane or designated as GOS UF membrane. In single electrolyte solutions with feed concentration at 100 ppm and initial pH of  $5.9 \pm 0.3$ , the rejection of iron and manganese were  $\geq 83\%$  and  $\geq 60\%$  respectively. Higher rejection was achieved as feed concentration increased to 1000 ppm for each ion with rejection of iron was  $\geq 90\%$  and manganese  $\geq 75\%$ . However, iron rejection was slightly decreased to  $\sim 78\%$ , while manganese rejection severely declined to  $\sim 22\%$  in multi-electrolytes filtration with feed concentration of 100 ppm iron and 50 ppm manganese. The feed pH for multi component system has significantly influenced iron and manganese rejection due to changes of the membrane surface properties. The rejection of iron and manganese by the negatively charged GOS UF membrane varied from 76% to 99% by adjustment of pH in the range of 3 to 11. Manganese rejection is mostly pH dependent with  $\geq 97\%$  rejection at feed pH  $\geq 9$ . This mixed matrix membrane with superior properties has the potential to remove iron and manganese to the desired extent for groundwater treatment.

**Keywords:** Polysulfone; Graphene oxide; Silver nanoparticles; Iron and manganese rejection; pH; Groundwater

### 1. Introduction

Heavy metals in water are always one of the main concerns especially for drinking water resources. This is because they are dangerous to human health and wildlife based on their toxicity, non-biodegradability and tendency

to accumulate in living organisms [1]. Most groundwater contains metals such as iron (Fe) and manganese (Mn) which naturally leaches from rocks and soils. Along with surface water, groundwater resources play a vital role in the production of clean and adequate drinking water supply all around the world. Iron and manganese are common metallic elements that exist together naturally especially in deeper wells [2]. The quantities of Mn that exists in groundwater

\*Corresponding author.

Presented at the 8th International Conference on Challenges in Environmental Science & Engineering (CESE-2015), 28 September – 2 October 2015, Sydney, Australia.

are commonly lower than Fe content. Neither one of these elements causes adverse health effects because both of them are essential to human diet as minerals. However, presence of excess amount of Fe and Mn resulted in metallic taste of water, slightly reddish colored water and rusty-brown stains on products like paper, cloths, and plastics [3]. In fact, these metallic elements in water may also promote growth of iron bacteria which form thick slime growths on the walls of piping system or on well screens that resulted in dirty water or also known as “red water”. In order to produce safe drinking water, the World Health Organization (WHO) suggested that Fe and Mn concentrations should be less than  $0.3 \text{ mg L}^{-1}$  and  $0.1 \text{ mg L}^{-1}$ , respectively [4].

Fe and Mn usually present in natural groundwater in their most soluble form as divalent ions,  $\text{Fe}^{2+}$  and  $\text{Mn}^{2+}$ . In soluble form, they are colorless in groundwater but when exposed to air, they oxidized and then turn into insoluble form of stable oxidation states of  $\text{Fe}^{3+}$  and  $\text{Mn}^{4+}$ , respectively. In fact, the soluble divalent ferrous and manganese ions can react with dissolved oxygen in groundwater and leave the water with brown-reddish color. Oxidation of iron as single electrolyte caused flocculation of orange precipitates. Whereas, manganese in single form of electrolyte formed blackish precipitates once they are oxidized.  $\text{Fe}^{2+}$  ions are more prone to oxidize when exposed to air at room temperature. However,  $\text{Mn}^{2+}$  ions are more stable and require a longer duration of aeration for its oxidation. Therefore, the most common method applied for removal of these metallic ions usually involved a combination with aeration as pre-treatment process. Natural groundwater in deeper wells consist of higher level of  $\text{Fe}^{2+}$  and  $\text{Mn}^{2+}$  because as the depth of aquifer increases, dissolved oxygen decreases indicating that waters containing dissolve oxygen will contain very little soluble Fe and Mn. Both divalent ions were less detected in shallow aquifer as trivalent ions were predominant iron and manganese contents in the aerated soil that is located within the unsaturated zone. Therefore, dissolved oxygen and water acidity play an important role in the quantity of Fe and Mn collected [5].

Several techniques have been applied to remove these metals from groundwater including ion-exchange and water softening, absorption by activated carbon, aeration and filtration, biosorption and ionic liquid extraction [5–9]. Recently, membrane technology including nanofiltration (NF) has been increasingly used in water treatment for producing drinking water resources. Numerous studies have been reported in investigating the ability of membrane filtration in water treatment [10–12]. Membrane technology is able to provide advantages not normally associated with conventional techniques such as smaller footprint, lower energy consumption and fewer man power requirements. In addition, other advantages of NF membranes are high retention of multivalent ions at lower operating pressure and thus, allowing operation at lower permeate flux. In water production industries or even in water treatment processes, it was reported that UF membranes were more preferable due to higher fluxes in comparison to NF membranes. However, UF membranes are more prone to macromolecules ions retention rather than multivalent ions. Therefore, this study was conducted to investigate the performance of nanohybrid PSF UF membrane in removal of Fe and Mn from groundwater.

In comparison to any other nylon or polymeric membranes, PSF is among the most attractive materials for

membranes fabrication. This is due to its excellent mechanical properties and higher water flux. However, its membrane surface is slightly hydrophobic which possibly may reduce surface wettability or self-cleaning effect for prolonged application. A number of studies have been reported on the reduction of the hydrophilicity of PSF membranes by embedding with metallic and non-metallic nanoparticles. Ng et al. [13] reported that a certain amount of polyvinyl alcohol (PVA) and  $\text{SiO}_2$  nanoparticles have been incorporated into the matrices of PSF membranes, which contributed to the enlargement in membrane pore size and thus increased the water permeability. Metallic nanoparticles such as silver (Ag) decorated with graphene oxide (GO) nanoplates have been embedded in PSF UF membrane matrices to obtain new novel nanohybrid graphene-oxide-silver membranes designated as GOS UF membrane. Mahmoudi et al. [14] reported that the modification has enhanced the GOS membrane performances in terms of higher water permeability, lower surface hydrophilicity as well as higher thermal and mechanical stability in comparison to other pure PSF UF membranes. In addition, the use of Ag with GO nanoplates that was synthesized using natural graphite powder according to Hummers method offers significant improvement in terms of providing more homogenous distribution of silver across the membranes and enhancement properties on antibacterial effect. GO as new polymer nanofillers with its unique properties such as a 2D carbon nanostructure, good thermo-mechanical stability and high specific surface area found increasing attention for used in combination with nanoparticles. As the GO nanoplates can be uniformly decorated with Ag nanoparticles, the agglomeration problem can possibly be resolved when used to produce nanohybrid GOS membranes.

The main aim of this work was to investigate the effect of concentration and pH of the feed solution on rejection mechanisms and solute-membrane interactions. Therefore, the fabricated UF nanohybrid membrane assigned as GOS membrane was characterized and further investigated on its performance to treat groundwater for drinking water resources. Performances of this membrane were discussed mainly on the metallic ions rejection and permeate flux. The potential of this membrane for groundwater treatment was compared with commercially available tight UF membranes. Further analysis such as surface morphology imaging was carried out using field emission scanning electron microscopy (FESEM) to support the rejection mechanism involved.

## 2. Materials and methods

### 2.1. Chemicals and membranes

All chemicals used were analytical grade with high purity and no further purification required. Ferrous chloride tetrahydrate ( $\text{FeCl}_2 \cdot 4\text{H}_2\text{O}$ ) was procured from HmbG® Chemicals and manganese chloride tetrahydrate ( $\text{MnCl}_2 \cdot 4\text{H}_2\text{O}$ ) was obtained from Bendosen Laboratory Chemicals. Both chemicals were used for preparation of synthetic groundwater by dissolving them as a single or multi component in ultra pure water with conductivity less than  $1 \mu\text{S cm}^{-1}$ . The synthetic groundwater was freshly prepared a day before filtration experiment and kept in a cold room to avoid the divalent ions from oxidized. Ferrous iron reagent powder (HACH Permachem®, USA) was used to determine the content of  $\text{Fe}^{2+}$

ions in permeate for each filtration. Manganese reagent set (HACH Permachem®, USA) that consists of buffer powder citrate type for Mn and sodium periodate were used to detect the concentration of Mn<sup>2+</sup> ions in permeate. Individual salt solutions of sodium chloride, sodium sulphate and calcium chloride (NaCl, Na<sub>2</sub>SO<sub>4</sub> and CaCl<sub>2</sub>) were freshly prepared using NaCl (Merck, Germany), Na<sub>2</sub>SO<sub>4</sub> and CaCl<sub>2</sub> (Sigma, USA) for salt rejection test. Low concentration of hydrochloric acid (HCl) and sodium hydroxide (NaOH) were used for pH adjustment on feed solution. All chemicals, solvents and reagents used were analytical grade with high purity.

Fabricated nanohybrid polysulfone (PSF) ultrafiltration (UF) membranes or named as GOS UF were employed in order to investigate the performance for groundwater treatment. Phase inversion method has been adopted for the fabrication of PSF-Ag-GO blend membranes. The casting solution has been prepared by dispersing the silver-graphene oxide nanoplates in 1/5 of the total N-methyl-2-pyrrolidinone (NMP). The polymer was mixed with the remaining NMP and kept in a silicon oil bath at a constant temperature of 80°C with a continuous stirring rate of 300 rpm. The nano-plates were ultrasonicated for 30 minutes before stirred in different beakers for 5 hours. The solution with nanoparticles was then added into the PSF/NMP mixture after a homogeneous solution was obtained. The final mixture was then ultrasonicated for another 30 minutes to produce a better dispersion of the nano-plates within the solution. Some of the casting solutions were then poured onto a clean glass plate and evenly dispersed using Filmographe Doctor Blade 360099003 (Braive Instrument, Germany) at a thickness of 0.2 mm. After 15 s of exposure of the casting solution on the glass plate to the air, the glass plate was immersed in ultrapure water at room temperature for the remainder of the phase-inversion process. The formed membranes were peeled off and rinsed with RO water for about 30 min. The specifications of the GOS UF membrane were as mentioned in Table 1.

## 2.2. Characterization of membranes

The wettability of membrane surfaces was analyzed by contact angle measurements using a static sessile drop method by Goniometer contact angle (Ramé-Hart, Model 290, Netcong, USA) with three series of measurement at three different spots. Images of top surface and cross-sectional morphologies of the fabricated membranes were provided by Zeiss SUPRA 55VP FESEM (Oberkochen, Germany). The instrument was equipped with an energy dispersive X-ray (EDX) analysis system to identify components that were filtered by the membranes. Liquid nitrogen was used to fracture the membranes which then required to be coated with platinum before the analysis of cross-sectional images. The membrane pure water permeability,  $L_p$  was determined by measuring using ultra-pure water at

operating pressures range of 1 to 5 bar and room temperature. Membranes were kept in pure water right after fabricated and compacted at 5 bar for 30 to 45 min prior to use.

Data of pure water flux  $J_v$  (L·m<sup>-2</sup>·h<sup>-1</sup>) was used to measure the membrane resistance  $R_m$  (m<sup>-1</sup>) as presented in the following Eq. (1). The applied pressure  $P$  (Pa) and the dynamic viscosity of water (kg·m<sup>-1</sup>·s<sup>-1</sup> or Pa·s) which is  $8.91 \times 10^{-4}$  at 25°C were also involved in the calculation.

$$R_m = \frac{\Delta P}{\mu J_v} \quad (1)$$

The overall porosity ( $\epsilon$ ) was calculated using a gravimetric method according to Eq. (2). The dried and wet membrane weight assigned as  $\omega_1$  and  $\omega_2$ , respectively. The surface area of membrane  $A$  (m<sup>2</sup>), the membrane thickness  $l$  and water density  $d_w$  (998 kg·m<sup>-3</sup>) were included for measurement.

$$\epsilon = \frac{\omega_2 - \omega_1}{A \times l \times d_w} \quad (2)$$

The pore sizes of fabricated membranes were calculated by Eq. (3). This calculation involved porosity data and using Guerout-Elford-Ferry equation. The water viscosity ( $8.9 \times 10^{-4}$  Pa·s), the volume of permeated pure water per unit time (m<sup>3</sup>·s<sup>-1</sup>) and operational pressure (0.4 MPa) were also used in the calculation.

$$\gamma_m = \sqrt{\frac{(2.9 - 1.75\epsilon)8\eta l Q}{\epsilon \times A \times \Delta P}} \quad (3)$$

In order to determine the surface zeta potential was measured using the Malvern Surface Zeta Potential Cell. The zeta potential of PSF membrane surface was measured in 0.1 mM NaCl at pH 4,7 and 9 using 300–350 nm latex particles as the tracer particles (DTS1235 Malvern UK).

## 2.3. Experimental set-up

A bench-scale dead-end stirred cell procured from Sterlitech Corporation, WA (Model HP4750) that houses a 49 mm diameter flat sheet membrane with effective area of 14.6 cm<sup>2</sup> was used for filtration experiment. The filtration setup comprises of a nitrogen gas tank, 300 mL stainless steel stirred cell and a precision balance (Sartorius AG, Germany, Model AX6202) connected to a data acquisition personal computer. The schematic diagram of the experimental apparatus is as illustrated in Fig. 1. Filtration experiments by using the selected membranes were conducted for 1 to 3 hours and permeate samples were collected for further water quality analysis of Fe<sup>2+</sup> and Mn<sup>2+</sup> ions using spectrophotometer (HACH, Model DR3900).

Table 1  
Specification of GOS nanohybrid membrane

Membrane	Polymer to nanoplate ratio	Ag-decorated GO concentration (wt%)	pH range at 25°C	Thickness (mm)	MWCO (kDa)
GOS	PSF:NMP:Ag-GO = 1:5.56:0.005	0.5	2–11	0.2	50

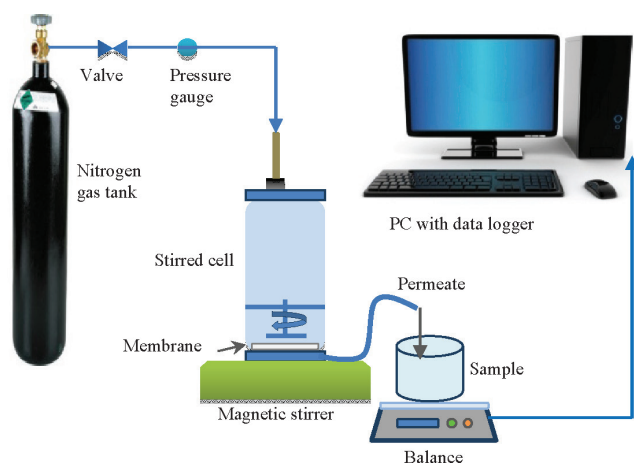


Fig. 1. Schematic diagram of dead-end stirred cell system.

Filtration experiments were performed to investigate the ability of the applied membranes based on permeability, flux and rejection using ultra pure water and synthetic samples of groundwater. All fabricated membranes were kept in ultra-pure water before used. The soaking step was considered as a wetting process for the membrane. Then, compaction of the membrane was conducted for 30 to 45 minutes by pressurizing the stirred cell with nitrogen gas at 5 bar without stirring. After compaction, the pure water permeability test was conducted. For determination of flux and rejection of synthetic groundwater, about 250 mL of feed solution was placed into the stirred cell and filtered for permeate collection. Data of permeate mass collected every 60 s was recorded by a software installed in the personal computer.

#### 2.4. Iron and manganese ion analysis

Permeate samples of  $\text{Fe}^{2+}$  and  $\text{Mn}^{2+}$  ions were analysed by using spectrophotometer (HACH, Model DR3900). Detection of  $\text{Fe}^{2+}$  and  $\text{Mn}^{2+}$  ions concentration in permeate were by APHA Standard Method 8146 and 8034 powder pillows, respectively. The detection limit for  $\text{Fe}^{2+}$  is 0.02 to 3.00  $\text{mg L}^{-1}$  whereas for  $\text{Mn}^{2+}$  is 0.1 to 20.0  $\text{mg L}^{-1}$ . The collected permeate after filtration process was checked for water quality analysis in identifying the best operating variables to meet the drinking water standards. Physico-chemical parameters were measured to investigate efficiency of membranes. Conductivity, pH and TDS were measured using Hanna Instrument HI2550, whereas turbidity were analyzed by using Turbidimeter (HA 2100AN). Color, in permeate were detected by using Spectrophotome-

ter (HACH, Model DR3900). All parameters were analyzed according to the APHA standard methods.

### 3. Results and discussion

#### 3.1. Surface properties of membrane

##### 3.1.1. Surface wettability

The surface wettability of membranes was measured by the static sessile drop method. The contact angle between pure water droplet and the clean surface of membrane is a measurement of wettability of membranes. Therefore, the tested membrane can be identified either it is a hydrophilic or hydrophobic membrane. A lower value of contact angle indicated that the membrane is more hydrophilic. A hydrophilic surface is obtained when the contact angle ( $\theta$ ) is lower than  $90^\circ$  and surface is completely wetted by water for a contact angle equal to  $0^\circ$  [15]. In this study, three series of measurement at three different spots of clean membranes were conducted a day after the samples were kept overnight in a desiccator. The average contact angle of the three clean membrane coupons for GOS membrane was measured at  $57^\circ \pm 1.5$ . Result showed that this membrane was more hydrophilic than the pure PSF UF ( $83.8 \pm 0.5$ ) membrane as reported by Mahmoudi et al. [14]. The contact angle of this membrane as presented in Fig. 2 was found reduced because of the addition of 0.5 wt% silver-decorated GO. The functional group of the silver-decorated GO has contributed to the reduction of interface energy of the mixed matrix membranes. Hydrophilicity of the fabricated GOS UF membrane revealed that it was suitable for further application in treating groundwater. However, the potential of this membrane in rejecting contaminants and meeting the drinking water standard was to be the main priority.

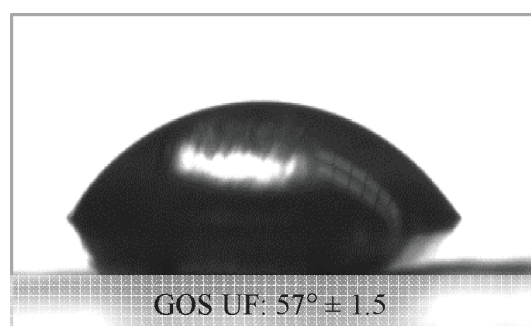


Fig. 2. Water drop contact angle of GOS UF membrane.

Table 2  
Characteristics of nanohybrid PSF and pure PSF ultrafiltration membranes

Membrane	Water flux <sup>a</sup> ( $\text{L.m}^{-2}.\text{h}^{-1}$ ) $\pm 0.5$	Membrane <sup>b</sup> resistance ( $\text{m}^{-1}$ ) $\pm 0.5$	Porosity <sup>b</sup> (%) $\pm 1.0$	Pore radius <sup>b</sup> (nm) $\pm 1.0$	Reference
GOS	29.3	16	61.7	8.8	Present study
Pure PSF	16.5	27	51.2	7.2	[14]

<sup>a</sup> Value obtained at pressure of 5 bar.

<sup>b</sup> Value obtained from experimental measurement.

### 3.1.2. Surface resistance and porosity

The surface resistance, overall porosity and pore radius of this membrane are summarized in Table 2. All measured data were calculated by Eqs. (1)–(3) as mentioned in earlier section and results were compared with the pure PSF membranes. The fabricated GOS membranes exhibited porosities higher than 50% and in comparison to the pure PSF membrane; it was 10% higher which is highly desirable in this work. Due to high porosity of GOS membrane, it was proven that the membrane surface resistance was reduced which could be ascribed by the addition of silver-decorated GO to the matrix of the membranes. Results also showed that only a small change on the pore radius of the GOS membranes in comparison to the pure PSF membranes.

### 3.1.3. Water flux

In water treatment industries, membranes with high water flux are more desirable for enhancement on water production. It is well-known that an improvement on surface wettability has a direct effect on the pure water flux. Therefore, it was expected that water flux by GOS membrane was higher than the PSF UF membrane as summarized in Table 2. Three different clean coupons of GOS membrane were used for measurement of pure water fluxes. The average volumetric water flux at applied pressure of 5.0 bar using this membrane was determined to be  $29.30 \pm 0.5 \text{ L}\cdot\text{m}^{-2}\cdot\text{h}^{-1}$ . From the observed results, these indicated that all coupons of GOS UF membranes conducted for this objective has the pure water permeability at  $5.86 \pm 0.5 \text{ L}\cdot\text{m}^{-2}\cdot\text{h}^{-1}\cdot\text{bar}^{-1}$ . This result showed that the separation layer of GOS membrane was highly permeable to water.

### 3.1.4. Surface morphology

Figs. 3(a) and 3(b) presented the FESEM images of surface and cross-sectional morphologies of pure PSF UF membrane. Whereas, Fig 3(c) and 3(d) were the FESEM images of the GOS UF membrane. The surface image of GOS UF membrane showed that no agglomerations of nanoparticles or graphene nanoplates could be observed as in comparison with the pure PSF UF membrane. Thus, the surface is smooth and silver-decorated GO was evenly distributed in the matrix of the membrane. The cross sectional image of the fabricated membrane demonstrated that it has a typical asymmetric morphology with finger-like pores linked by a sponge walls. Results indicated that the structures of membrane cross sections were not affected by the addition of silver-decorated GO.

Figs. 3(e) and 3(f) presented the EDX spectrum and mapping images of the fabricated membrane. The peaks located at 2.65 and 2.984 verified the presence of silver nanoparticles in the membrane matrices. In order to study the distribution pattern of the Ag-GO in the structure of the membrane, EDX in mapping mode was used. Based on the scanning result, an excellent distribution of the silver nanoparticles in the membrane matrix was observed. This suggests that the decoration of silver on the graphene oxide can prevent nanoparticles agglomeration and lead to an even distribution of the silver in the structure of the membrane. Therefore, this can enhance the oligodynamic effect across the skin of the membrane.

### 3.2. Flux behaviour and fouling tendency

Fig. 4 showed fluxes trend by using the GOS UF membrane. In Fig. 4(a), it was found that synthetic groundwater fluxes were slightly lower than the pure water fluxes for permeability test at applied pressure in the range of 1 to 5 bar. In this part, synthetic groundwater with multi-electrolytes was used with concentration of 100 mg Fe/L and 50 mg Mn/L. It was prepared without addition of any background electrolytes. Divalent ions of  $\text{Mn}^{2+}$  typically exist in natural groundwater at concentration that is much lower than  $\text{Fe}^{2+}$ . In this case, the co-exist of Fe:Mn at 100:50 mg  $\text{L}^{-1}$  were chosen mainly in order to further investigate the ability of GOS UF membrane for co-removal of iron and manganese at high concentration. The initial measured pH of the feed solution before used was  $5.9 \pm 0.3$  with conductivity at  $209.7 \pm 0.5 \mu\text{S}$ . Fig. 4(b) presented the normalized flux of synthetic groundwater at applied pressure of 5 bar for filtration process within two hours at stirring rate of 500 rpm. This result showed that no flux decline within the operating period and average volumetric flux was found at  $26.3 \pm 2.5 \text{ L}\cdot\text{m}^{-2}\cdot\text{h}^{-1}$ . The final pH measured after the filtration experiment was  $6.8 \pm 0.3$  and this measurement indicated that the water quality for pH has complied with the standard of drinking water by WHO. Furthermore, rejections of the divalent metallic ions at this point were 92.4% and 82.3% for  $\text{Fe}^{2+}$  and  $\text{Mn}^{2+}$  ions, respectively. At this condition, the GOS membrane was considered to be performing well despite the qualities of both ions in permeate were still above the drinking water standards which were 7.6 and 8.9 mg  $\text{L}^{-1}$  for Fe and Mn, respectively. According to the allowable level of both metallic ions in water, results achieved in this section were 96% ( $\text{Fe}^{2+}$ ) and 88% ( $\text{Mn}^{2+}$ ) were reaching the drinking water standard.

### 3.3. Effect of feed concentrations

The Department of Mineral and Geoscience, Malaysia has reported that concentrations of Fe in natural groundwater sources were typically range from 0.7 to 94 mg  $\text{L}^{-1}$ , with an average concentration of 15.6 mg  $\text{L}^{-1}$ . Manganese typically presents in lower concentration in the range from less than 0.1 to 2.7 mg  $\text{L}^{-1}$ , with an average concentration of 0.43 mg  $\text{L}^{-1}$ . In order to determine the effectiveness of using the selected membrane for treating groundwater with higher concentration range of metal elements, synthetic water at various concentrations of  $\text{Fe}^{2+}$  and  $\text{Mn}^{2+}$  were used for further investigation. The effect of initial feed concentration on the rejection of these metallic ions is presented in Fig. 5(a). Filtration experiments were conducted at applied pressure of 5 bar, ambient temperature and stirring rate of 500 rpm. For this part, performance of the GOS membranes were tested by using a single electrolyte in the synthetic groundwater.

Results showed that rejection of  $\text{Fe}^{2+}$  and  $\text{Mn}^{2+}$  ions increased with increasing initial feed concentrations from 100 to 1000 mg  $\text{L}^{-1}$ . Very high observed rejection of  $\text{Fe}^{2+}$  values from 82.6% to 92.6% were obtained by using this membrane, indicating that it has very good separation properties for metallic ions removal. It was observed that a similar trend was also depicted for  $\text{Mn}^{2+}$  removal. The rejection of  $\text{Mn}^{2+}$  ions using this membrane increased from 61.1% to 75.9%. These results confirmed that the presence of  $\text{Fe}^{2+}$  and  $\text{Mn}^{2+}$  ions in synthetic groundwater even at very

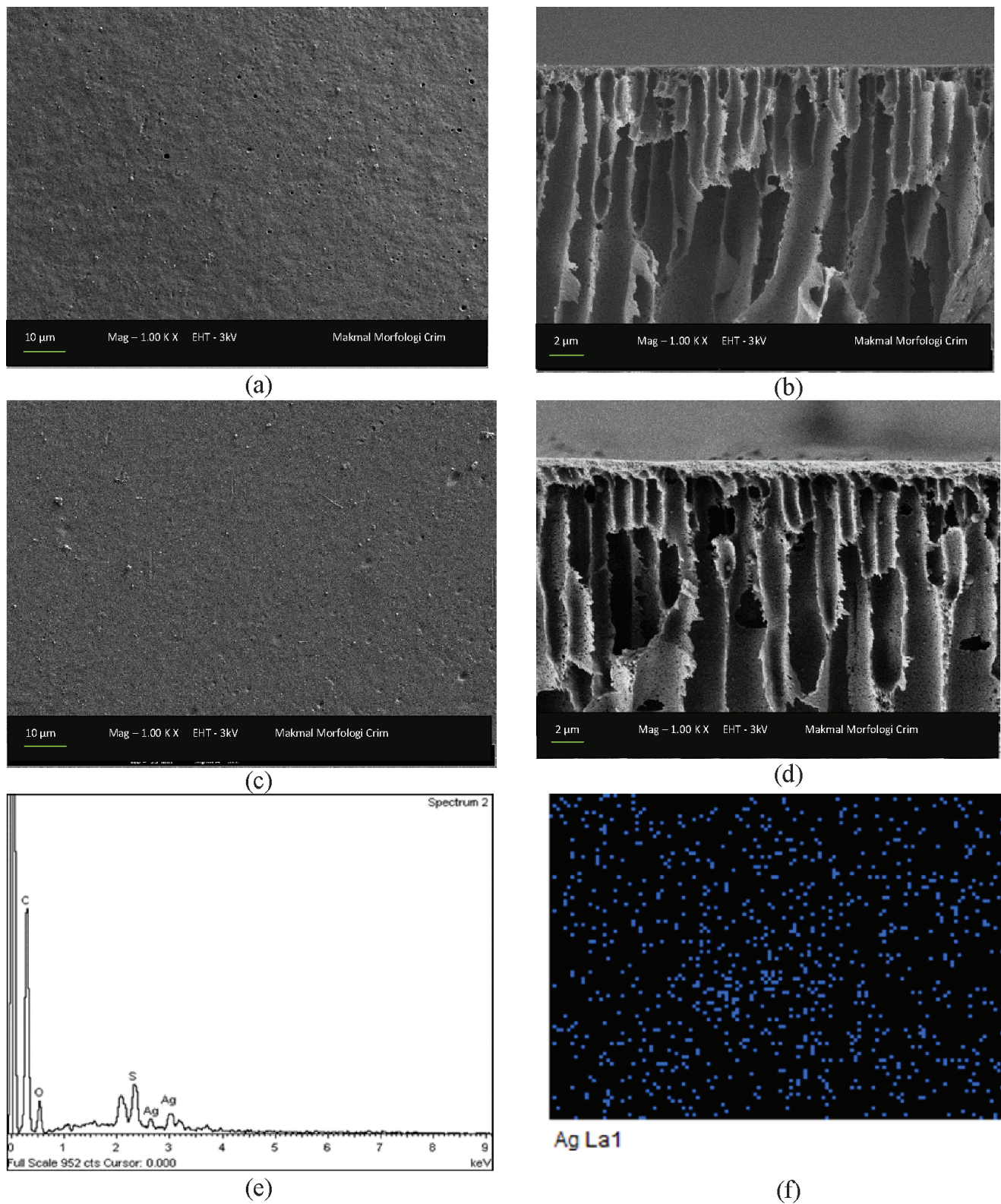


Fig. 3. FESEM images of (a) surface, (b) cross sectional morphology of clean pure PSF membrane, (c) surface, (d) cross sectional morphology with (e) EDX spectrum and (f) mapping of clean GOS UF (0.5 wt% silver decorated graphene oxide) membrane.

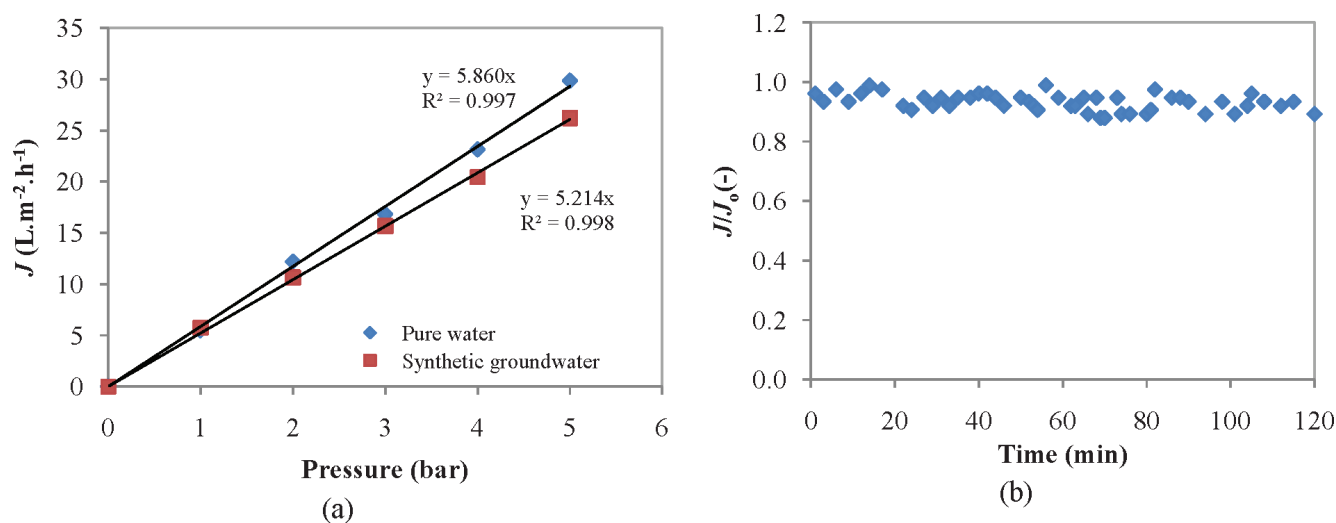


Fig. 4. (a) Flux for pure water and synthetic groundwater at various applied pressures and (b) normalized flux of filtration of synthetic groundwater at operating conditions: 100 mg Fe/L and 50 mg Mn/L, 5 bar, pH 6.8, 25°C and 500 rpm stirring rate.

high concentration were effectively rejected by the GOS membrane. It was clearly determined that this membrane has high ability to remove both metallic ions and suitable for further inspection using natural groundwater. However, it should be noted that the metals concentration in permeate were not below the acceptable limits for drinking water standards. Therefore, further investigation by other operating conditions was suggested to optimize the performance of GOS membranes at high concentration of the metallic ions in the feed solutions. The findings on Fe and Mn rejection percentage revealed that the selected GOS UF membranes have an outstanding performance in comparison to other commercial UF membranes or other treatment methods [6,8,11,16].

Separation mechanism by UF and NF membranes involved both steric (sieving) effects and electrical (Donnan) effects [17]. UF membranes are effectively able to reject macromolecules and allow the monovalent ions to pass through. For this study, both metallic ions were proportionally rejected with increasing metal concentration in the aqueous solution. Thus, by considering only the corresponding charge effects, both metallic ions rejection were expected to increase with increasing feed concentration. Increase in the ionic strength of a solution may cause a decrease in the pore size of the membranes resulting in an increase of solute rejection [18]. Similar finding has been discovered by Nguyen et al. [19] as they reported that at high ionic strength, the electrostatic repulsion between nearby negatively charged carboxylates was reduced because of double layer compression and charge screening at the solution-pore wall interface that tend to cause a decrease in pore size and increase on arsenic rejection. Therefore in this study, slight increase of both metallic ions rejection at high ionic strength was believed to have been affected by electrostatic interactions of solute with the negatively charged GOS UF membrane due to the decrease of pore size (volume) of membrane.

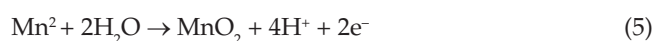
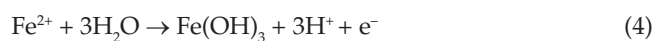
The performance of the GOS membranes was also tested by using multi electrolyte in the synthetic groundwater. For this case, a mixture of 100 mg Fe/L and 50 mg Mn/L was used in the feed solutions at initial pH of

$6.3 \pm 0.3$ . Results depicted in Fig. 5(b) showed that rejection rates for both metallic ions were slightly decreased in multi components solution. The reduction of performance based on rejection was found to be less than 6% which indicated that there were less affinity of solute-solute interaction involved, regardless the filtration was by single or multi components system.

### 3.4. Effect of pH on solute and membrane

#### 3.4.1. Feed Solution

The prepared synthetic groundwater was added with low concentration at 0.1 M of hydrochloric acid (HCl) or sodium hydroxide (NaOH) in order to adjust the pH of feed solutions in the range of 3 to 11. Initial pH of FeCl<sub>2</sub> and MnCl<sub>2</sub> feed solution was  $5.9 \pm 0.3$ . At this condition, both divalent metallic ions were soluble in water. At this point, the prepared synthetic groundwater samples consist of either Fe<sup>2+</sup> and Mn<sup>2+</sup> ions were colourless as sample A in Fig. 6(a). By increasing the feed pH, soluble divalent ions were slowly oxidized to become insoluble and stable ions according to the following equations;



Therefore, pH has affected solubility of solute. These metallic divalent ions were less soluble at higher value of pH. Insoluble trivalent ferric ions, Fe<sup>3+</sup> or known as iron solid commonly occurs as colourful bright reddish-yellow to yellowish-brown stains as in sample B in Fig. 6(a). Once sample B was left for 20 to 30 minutes, precipitate of iron hydroxide (Fe(OH)<sub>3</sub>) settled down as sediment at the bottom of the sample cell as shown in Fig. 6(b). The stability of Fe ions depend not only on pH but also on the activity of electrons. The occurrence and behaviour of Mn is not

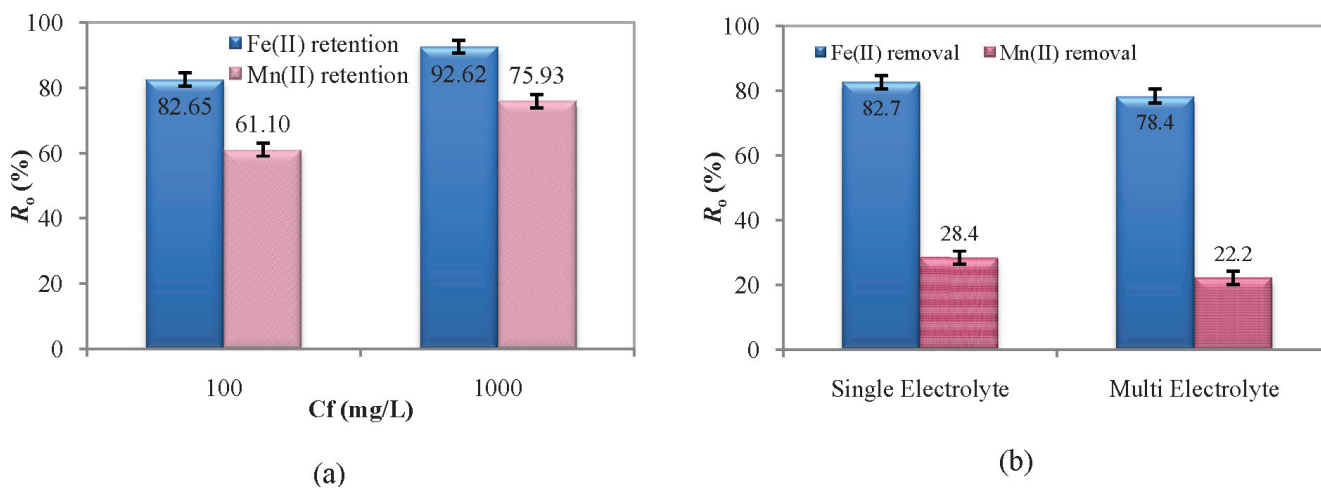


Fig. 5. Iron and manganese rejection at (a) various feed solution concentrations and (b) single or multi components system.

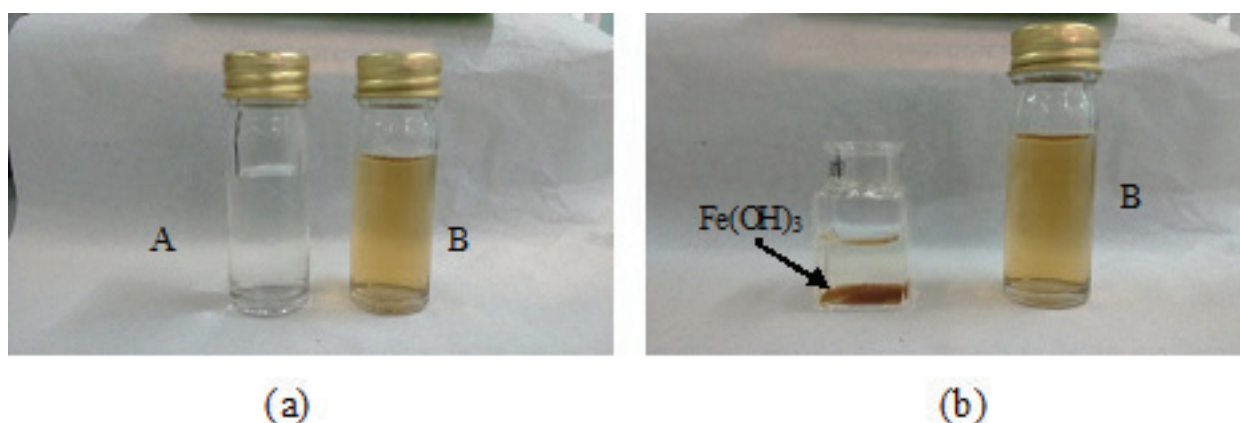


Fig. 6. Physical properties of 100 mg Fe/L of feed solution (a) with initial pH at 6.5 (sample A), adjusted pH at 9.3 (sample B) and (b) when flocs of  $Fe(OH)_3$  formed.

similar to Fe. It was found that  $Fe^{2+}$  was more rapidly and easily oxidized than  $Mn^{2+}$ . Precipitate of  $MnO_2$  requires a longer duration for sedimentation. The precipitations of  $Fe(OH)_3$  and  $MnO_2$  were due to the feed solution having bigger size of particles formed once the pH increased. Different species of same solute have different characteristics such as size and charge, which significantly affect rejection mechanism [20]. Therefore, size exclusion was expected to become the dominant rejection mechanism that has been significantly influenced at higher pH of the feed solutions.

Furthermore, divalent ion  $Fe^{2+}$  is predominant at  $pH < 6.8$  while the trivalent  $Fe^{3+}$  dominates at  $pH$  above than 6.8. Therefore, more divalent ferrous ions were transformed to the trivalent ferric ions when  $pH$  increased. For the case of manganese, the divalent  $Mn^{2+}$  is predominant at  $pH < 9.3$  and thus, the multivalent  $Mn^{4+}$  dominates at  $pH$  above than 9.3. The increase in  $pH$  will help in the oxidation of iron and if it is raised high enough it will favor the oxidation of manganese. Very high  $pH$  is required for the oxidation of soluble manganese without adding any strong oxidant. The oxidation rates are faster at high  $pH$  values and become slower at low  $pH$ . In practice, the removal of dissolved  $Fe^{2+}$

and  $Mn^{2+}$  from groundwater used to accomplish by the oxidation and precipitation. Mansoor et al [2] reported that the removal process of these two elements from groundwater is affected by the different chemical and physical characteristic of water including  $pH$ , total organic carbon (TOC) and concentration of dissolved oxygen. The occurrence and concentration of Fe and Mn in groundwater in particular were controlled by water chemistry ( $pH$ , redox potential (Eh), dissolved oxygen (DO) and dissolved organic carbon (DOC).

Fig. 7 showed the zeta potential of both solutes at various  $pH$  of feed solutions. The isoelectric point (IEP) of iron and manganese was found at  $pH$  7.8 and  $pH$  3.3, respectively. At this point, solutes are uncharged and the rejection mechanism was mainly depend on sieving effect. Results in Figs. 7(a) and 7(b) showed that Mn is more negatively charged than Fe as  $pH$  increased. Therefore, it was expected that electrostatic repulsion between membrane and solute became stronger with increasing  $pH$  when a negatively charged membrane is used. The graphene oxide and silver decorated graphene are both negatively charged [21]. The hydroxyl, epoxide, carbonyl and carboxyl groups of the graphene oxide resulting



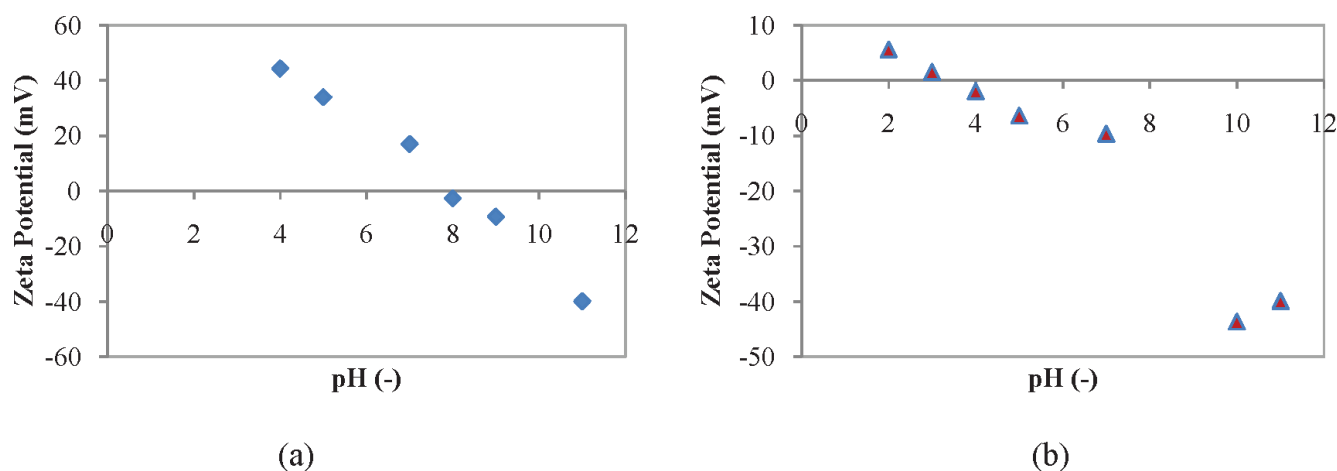


Fig. 7. Zeta potential of solute (a) Fe (b) Mn.

in a negatively charged surface [22]. This is a well known concept reported by many authors.

#### 3.4.2. Permeate quality

Fig. 8 presents the permeate concentration measured after filtration by using multi components feed solution with 100 mg Fe/L and 50 mg Mn/L at adjusted pH in the range of 3 to 11. Results showed that at this pH range, the concentration of metal ions detected in permeate decreased with increasing pH. This result proved that removal of both metallic ions from synthetic groundwater increased with increasing pH of the feed solution.

For Fe removal by GOS membrane at pH 7, 9 and 11, permeate concentration measured were well below than the acceptable limit for drinking water standard by WHO which were 0.17, 0.24 and 0.08 mg Fe/L, respectively. These results indicated that Fe rejection was successful at pH above than 7 and poor rejection of Fe when feed solution pH was adjusted below than 7. Thus, results proved that pH has importantly impacted Fe removal as also reported by other scholars [20,23,24]. The feed pH may change the nature of the membrane surface charge and pore size, as well as the dissolved metal species and therefore can affect the membrane separation efficiency [25]. Between pH 3 and 7, almost all Fe were present as soluble  $\text{Fe}^{2+}$ . Higher than pH 8, Fe is predominantly present as insoluble  $\text{Fe}^{3+}$  and easily precipitate as  $\text{Fe}(\text{OH})_3$  on the surface of membrane. Therefore, Fe removal at this point was mainly by size exclusion.

For Mn removal with feed concentration at 50 mg Mn/L, it was found that the best quality of permeate occurred when using feed solution at pH 9 with detected permeate concentration at 0.35 mg Mn/L as shown in Fig. 8. However, it was considered as unsatisfactory result as for drinking water since the acceptable value should be at least 0.1 mg Mn/L. Poor quality of permeate at below than pH 11 can be attributed to the effect of concentration polarization. The occurrence and behavior of Mn is not similar to Fe, as  $\text{Fe}^{2+}$  ions were easily and rapidly oxidized than  $\text{Mn}^{2+}$  ions. At higher than pH 9, Mn is slowly exist as stable  $\text{Mn}^{4+}$  and insoluble as  $\text{MnO}_2$  which then precipitate on the surface of membrane.

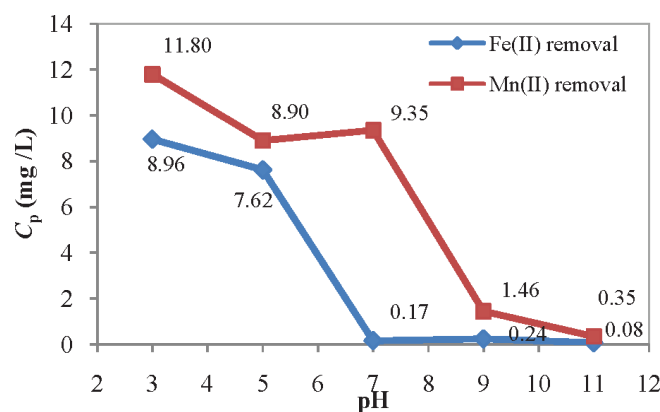


Fig. 8. Effect of pH on permeate concentration for filtration of Fe and Mn.

At this point, Mn removal could be attributed solely by size exclusion. Between pH 3 and 7, Mn exist as soluble  $\text{Mn}^{2+}$  and thus, easily permeate and pass through membrane pores. As the result, poor rejection occurred especially at pH 3 with high value of permeate concentration at 11.8 mg Mn/L was detected. In acidic feed solution, membrane pores could be expanded. At this point, low rejection at pH 3 explained that solute-membrane interaction is the main mechanism and dominated by the nature of the membrane pores.

#### 3.4.3. Solute rejection

Fig. 9(a) presents the effect of feed pH on Fe and Mn rejection by using GOS membrane. In general, as the pH increased from 3 to 11, the rejection of both metallic ions were increased. This can be mainly caused by the solute-membrane charges interactions and also due to the size exclusion effect. It was obviously shown that the rejection of Fe at various feed pH were higher than Mn. The main reason for this behaviour was probably because of  $\text{Fe}^{2+}$  ions were easily oxidized at higher pH and  $\text{Mn}^{2+}$  ions were more stable which contributed to having a longer period for oxidation. Lower rejection of Mn than Fe could

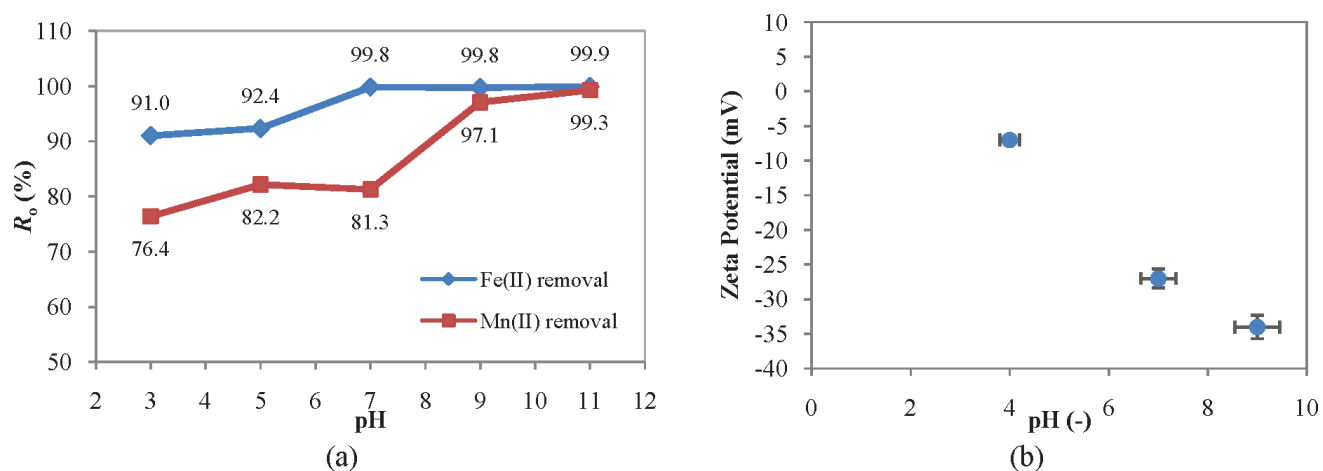


Fig. 9. Rejection (a) of Fe and Mn using 100 mg Fe/L and 50 mg Mn/L, 5 bar, 25°C with 500 rpm stirring rate and zeta potential (b) of GOS UF membrane as a function of pH.

be attributed solely to the electrostatic effect interaction between membrane material and  $Mn^{2+}$  ions. Kabsch-Korbutowicz and Winnicki [16] reported that retention of manganese compound from  $MnCl_2$  at pH 6.6 was dominated by  $Mn^{2+}$  ions as oxidation used to occur above than pH 9. In addition, the ferrous chloride rejection was higher than manganese chloride rejection as depicted in Fig. 8(a), and this higher rejection of ferrous salt was determined by the higher hydration energy of  $Fe^{2+}$  in comparison to  $Mn^{2+}$ . The molar Gibbs energies of hydration of ions  $Fe^{2+}$  and  $Mn^{2+}$  is  $-1840$  and  $-1760$   $kJmol^{-1}$  [26], respectively. Similar results which highlighted the increase in the cation rejection with increasing hydration energy were obtained by Gherasim et al. [27] and Mehiguene et al. [28].

The pH of feed solution may change the nature of the membrane surface charge and pore size, as well as the dissolved metal species and therefore can affect the membrane separation efficiency. The GOS membrane has reached higher rejection rate for both metals in comparison by using other commercial UF membranes. Similar findings for  $Fe^{2+}$  ions removal has previously been reported by other scholars [6,29]. Regarding to  $Mn^{2+}$  ions, De Munari and Schäfer [30] reported that PA-NF membrane has achieved more than 95% of rejection at pH 7. In Fig. 8, Mn rejection at pH 9 has increased very well to >95% from 76% rejection at pH 3. This was mainly because of changes of solute to a stable form which easier to be removed by membrane as further explained in the earlier section. The good rejection at this condition was mainly contributed by solute-membrane charge interactions. The charge of solute influenced the extent of rejection by membranes though the precise mechanism of rejection will depend upon the particular membrane in use [31].

The zeta potential of GOS UF membrane as a function of pH is presented in Figure 9(b). Measurement of this parameter at pH 4, 7, and 9 resulted with negative values of zeta potential indicated that the GOS membrane is more negatively charged with increase of pH. The GOS membrane had a positive charge below pH 2.5, and passed through the IEP at approximately pH 2.5. Thus, solute charge repulsion was less important at this point since the membrane was at zero charge. It was believed that rejection of both ions at this point

(IEP) was dominantly controlled by sieving effect and co-ions as the surface charge of membrane is more rejected at pH higher than 2.5. As reported in earlier section, the IEP of  $Fe^{2+}$  and  $Mn^{2+}$  were found at pH 7.8 and 3.3, respectively. Therefore,  $Mn^{2+}$  ions were more prone to be removed based on electrostatic charge repulsion as it was more negatively charged than  $Fe^{2+}$  at pH higher than 3.3. However, removal of Fe was found higher than Mn as depicted in Figure 9(a) was believed due to the hydration energy of  $Fe^{2+}$  and  $Mn^{2+}$ . The ion filtration resulting from the electrostatic interactions between ions and membrane surface charge is based on the Donnan exclusion mechanism [32]. In this mechanism, the co-ions (which have the same charge of the membrane) are repulsed by the membrane surface and to satisfy the electroneutrality condition, an equivalent number of counter-ions is retained [33].

Results in Fig. 9 indicated that removal of  $Fe^{2+}$  at pH above than 7 was dominated by both size exclusion and electrostatic charge repulsion. Whereas, at pH below than 7 the removal mechanism was solely due to the size exclusion (sieving effect) mechanism. Retentions of  $Mn^{2+}$  ions at pH 3, 5 and 7 were solely attributed by electrostatic charges repulsion. At pH above than 3,  $Mn^{2+}$  ions are co-ions to the negatively charged GOS UF membrane. Therefore, manganese

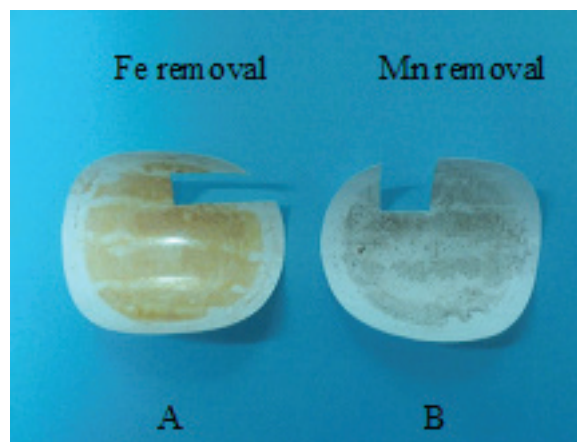


Fig. 10. Visualization on physical quality of fouled GOS UF membrane for filtration at 5 bar and pH9.

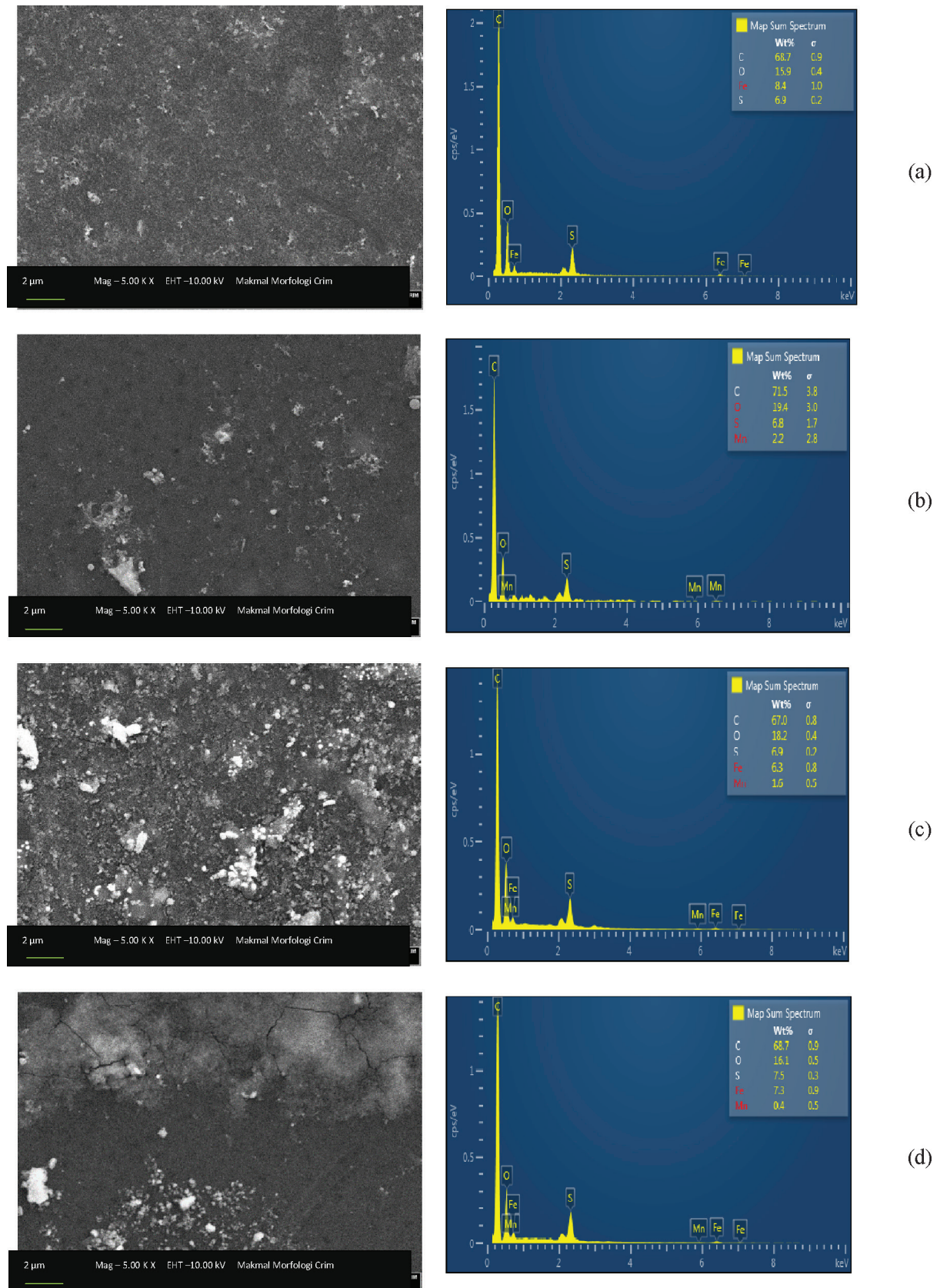


Fig. 11. FESEM images of fouled GOS UF membranes with EDX analysis for filtration using (a) 100 ppm Fe, (b) 100 ppm Mn, (c) 100 ppm Fe-50 ppm Mn at pH 5 and (d) 100 ppm Fe-50 ppm Mn at pH 7.

removal by this membrane was expected to be higher within pH range of 3 to 11. Morgan [34] in his study on oxidation rate of  $Mn^{2+}$  has discovered that this metallic ion was relatively slow oxidized at pH values below than 9.5. For this reason, it was found that higher retention was obtained at pH 9 and 11 since the size exclusion and electrostatic repulsion were involved as the main rejection mechanism.

### 3.5. Surface morphology analysis

Fig. 10 presented an image of fouled GOS membranes for filtration of single metal component in synthetic groundwater at pH 9. From visual observation, brown-orengy cake layer become visible on top surface of membrane A, that resulted from Fe removal. Whereas, blackish cake layer formed on the surface of membrane B after filtration with synthetic groundwater solution with Mn ions. The cake layer formed mainly because of precipitation of  $Fe(OH)_3$  and  $MnO_2$  as explained in the earlier section. Fig. 11(a) and 11(b) showed the FESEM images of  $Fe(OH)_3$  and  $MnO_2$  precipitation, respectively. Larger size of crystalline  $MnO_2$  precipitate were clearly seen on top surface of GOS membrane. Bordoloi et al. [35] reported that the SEM image with EDS analysis of arsenic and iron removal from groundwater by oxidation-coagulation at optimized pH revealed that the sorption of As onto the poorly crystalline precipitate of  $Fe(OH)_3$  and existence of a small amount of  $MnO_2$ .

The FESEM images of the precipitate obtained in the presence of Fe and Mn for filtration of multi component by using GOS membranes at adjusted pH of feed solutions were depicted in Fig. 11(c) and 11(d). The precipitates of  $Fe(OH)_3$  and  $MnO_2$  at pH 5 were observed on the surface of GOS membrane as presented by Fig. 11(c). Whereas, Fig. 11(d) indicated that the precipitate of both metallic elements using feed solution at pH 7. Results showed the membrane surface images of GOS membranes with aggregated large regularly shaped particles unevenly precipitate of  $MnO_2$  stable crystallinity. In comparison to  $Fe(OH)_3$ ,  $MnO_2$  was found more stable especially at pH higher than 8.

## 4. Conclusions

The rejection mechanism using GOS UF membranes in removal of Fe and Mn from synthetic groundwater were identified and evaluated in this study. The main focus of this paper was to investigate the influence of feed solution pH on solute and membrane interactions. The efficiencies of the GOS UF membranes were assessed based on permeability, water flux and rejection capabilities at 5 bar and feed solution pH ranged at 3 to 11. The rejection rates for metal components (Fe and Mn) using these membranes were significantly influenced by the adjustment on pH of the feed solutions. Results proved that GOS membrane had efficiently rejected  $Fe^{2+}$  and  $Mn^{2+}$  ions to the allowable value for drinking water based on WHO standards. Excellent separation performance of this membrane especially at pH above than 7 was mainly due to its effective separation layer of membrane structure and the electronegativity of membrane surfaces.

The contribution of solute-membrane charge interactions was determined to have significant influence as a function of the pH of feed solution. Increases of pH lead to a higher efficiency of Fe and Mn rejections by this membrane. Higher pH of the feed solution contributed to transformation of soluble divalent  $Fe^{2+}$  and  $Mn^{2+}$  ions to insoluble  $Fe^{3+}$  and  $Mn^{4+}$  ions which were more stable. Therefore, they were easily flocculated and precipitated on membrane surfaces. Furthermore, the adjustment of pH has also affected solute and membrane surface charges that contributed to electrostatic interaction which enhanced both metallic ions removal. Higher rate of removal especially for  $Mn^{2+}$  ions was mainly attributed by the GOS UF membranes that were characterized as negatively charged membrane at pH above than 2.5. Size exclusion and electrostatic charge repulsion were the main rejection mechanisms involved for Fe and Mn removal at pH values higher than 7 or 9. In conclusion, the nanohybrid PSF UF membrane used in this study has high potential to treat groundwater for drinking water resources even though at high concentration of Fe and Mn. The improved characteristics of this membrane in terms of providing higher flux, higher hydrophilicity and antibacterial properties were expected to become the advantages towards application of membrane technology in water treatment processes.

## Acknowledgements

The authors would like to thank Universiti Kebangsaan Malaysia by the grant ICONIC-2013-002 for financial supports. Additionally, the first author is gratefully wished special thanks to the National Defence University of Malaysia for funding the scholarship.

## References

- [1] K.H. Lanouette, Heavy Metals Removal, Chem. Eng. (New York), 84 (1977) 73–80.
- [2] M. Ahmad, Iron and Manganese removal from groundwater, University of Oslo, 2012.
- [3] R.H. Marchovecchio, J.E. Botte, S.E. Freiji, Heavy Metals, Major Metals, Trace Elements, In: Handb. Water Anal., CRC Press, 2011.
- [4] WHO, Guidelines for drinking-water quality, In: Recommendations, Vol.1, 3<sup>rd</sup> ed., World Health Organization, Geneva, (2008) 390–399.
- [5] S. Chaturvedi, P.N. Dave, Removal of iron for safe drinking water, Desalination, 303 (2012) 1–11.
- [6] A. Jusoh, W.H. Cheng, W.M. Low, A. Nora'aini, M.J. Megat Mohd Noor, Study on the removal of iron and manganese in groundwater by granular activated carbon, Desalination, 182 (2005) 347–353.
- [7] D. Ellis, C. Bouchard, G. Lantagne, Removal of iron and manganese from groundwater by oxidation and microfiltration, Desalination, 130 (2000) 255–264.
- [8] A. Binti Abdul Kadir, N.B. Othman, N.M. Azmi, Potential of using *Rosa Centifolia* to remove iron and manganese in groundwater treatment, Int. J. Sustain. Constr. Eng. Technol., 3 (2012) 70–82.
- [9] N.H. Hussin, I. Yusoff, Y. Alias, S. Mohamad, N.Y. Rahim, M.A. Ashraf, Ionic liquid as a medium to remove iron and other metal ions: a case study of the North Kelantan Aquifer, Malaysia, Environ. Earth Sci., 71 (2013) 2105–2113.

- [10] J.H. Potgieter, R.I. Mccrindle, Z. Sihlali, R. Schwarzer, N. Basson, Removal of iron and manganese from water with a high organic carbon loading Part I: the effect of various coagulants, *Water, Air Soil Pollut.*, 162 (2005) 49–59.
- [11] K.H. Choo, H. Lee, S.J. Choi, Iron and manganese removal and membrane fouling during UF in conjunction with prechlorination for drinking water treatment, *J. Memb. Sci.*, 267 (2005) 18–26.
- [12] J.L. Lin, C. Huang, J.R. Pan, Y.S. Wang, Fouling mitigation of a dead-end microfiltration by mixing-enhanced preoxidation for Fe and Mn removal from groundwater, *Colloids Surfaces A Physicochem. Eng. Asp.*, 419 (2013) 87–93.
- [13] L.Y. Ng, C.P. Leo, A.W. Mohammad, Optimizing the incorporation of silica nanoparticles in polysulfone/poly(vinyl alcohol) membranes with response surface methodology, *J. Appl. Polym. Sci.*, 121 (2011) 1804–1814.
- [14] E. Mahmoudi, L. Yong, M.M. Ba-abbad, A.W. Mohammad, Novel nanohybrid polysulfone membrane embedded with silver nanoparticles on graphene oxide nanoplates, *Chem. Eng. J.*, 277 (2015) 1–10.
- [15] H. Kelewou, A. Lhassani, M. Merzouki, P. Drogui, B. Sellamuthu, Salts retention by nanofiltration membranes: physicochemical and hydrodynamic approaches and modeling, *Desalination*, 277 (2011) 106–112.
- [16] M. Kabsch-Korbutowicz, T. Winnicki, Application of modified polysulfone membranes to the treatment of water solutions containing humic substances and metal ions, *Desalination*, 105 (1996) 41–49.
- [17] A.W. Mohammad, R. Othaman, N. Hilal, Potential use of nanofiltration membranes in treatment of industrial wastewater from Ni-P electroless plating, *Desalination*, 168 (2004) 241–252.
- [18] J. Cho, G. Amy, J. Pellegrino, Membrane filtration of natural organic matter: factors and mechanisms affecting rejection and flux decline with charged ultrafiltration (UF) membrane, *J. Memb. Sci.*, 164 (2000) 89–110.
- [19] C.M. Nguyen, S. Bang, J. Cho, K.W. Kim, Performance and mechanism of arsenic removal from water by a nanofiltration membrane, *Desalination*, 245 (2009) 82–94.
- [20] L.A. Richards, M. Vuachère, A.I. Schäfer, Impact of pH on the removal of fluoride, nitrate and boron by nanofiltration/reverse osmosis, *Desalination*, 261 (2010) 331–337.
- [21] M. Wang, J. Oh, T. Ghosh, S. Hong, G. Nam, T. Hwang, J.D. Nam, An interleaved porous laminate composed of reduced graphene oxide sheets and carbon black spacers by *in situ* electrophoretic deposition, *RSC Adv.*, 4 (2014) 3284.
- [22] J. Lee, H.R. Chae, Y.J. Won, K. Lee, C.H. Lee, H.H. Lee, I.C. Kim, J. Lee, Graphene oxide nanoplatelets composite membrane with hydrophilic and antifouling properties for wastewater treatment, *J. Memb. Sci.*, 448 (2013) 223–230.
- [23] S. Bordoloi, S.K. Nath, S. Gogoi, R.K. Dutta, Arsenic and iron removal from groundwater by oxidation-coagulation at optimized pH: laboratory and field studies, *J. Hazard. Mater.*, 260 (2013) 618–626.
- [24] M.R. Muthumareeswaran, G.P. Agarwal, Feed concentration and pH effect on arsenate and phosphate rejection via polyacrylonitrile ultrafiltration membrane, *J. Memb. Sci.*, 468 (2014) 11–19.
- [25] B.A.M. Al-Rashdi, D.J. Johnson, N. Hilal, Removal of heavy metal ions by nanofiltration, *Desalination*, 315 (2013) 2–17.
- [26] Y. Marcus, Thermodynamics of solvation of ions, *J. Chem. Soc. Faraday Trans.*, 87 (1991) 2995–2999.
- [27] C.V. Gherasim, P. Mikulášek, Influence of operating variables on the removal of heavy metal ions from aqueous solutions by nanofiltration, *Desalination*, 343 (2014) 67–74.
- [28] K. Mehiguene, Y. Garba, S. Taha, N. Gondrexon, G. Dorange, Influence of operating conditions on the retention of copper and cadmium in aqueous solutions by nanofiltration: experimental results and modelling, *Sep. Purif. Technol.*, 15 (1999) 181–187.
- [29] A. De Munari, A.J.C. Semiao, B. Antizar-Ladislao, Retention of pesticide Endosulfan by nanofiltration: influence of organic matter-pesticide complexation and solute-membrane interactions, *Water Res.*, 47 (2013) 3484–3496.
- [30] A. De Munari, A.I. Schäfer, Impact of speciation on removal of manganese and organic matter by nanofiltration, *J. Water Supply Res. Technol.*, 59 (2010) 152.
- [31] T.D. Waite, Chemical speciation effects in nanofiltration separation, In: T.D. Schäfer, Andrea I., Fane, A.G., Waite (Ed.), *Nanofiltration-Principles Appl.*, First, Elsevier B.V., (2005) 148–168.
- [32] J. Schaep, B. Van der Bruggen, C. Vandecasteele, D. Wilms, Influence of ion size and charge in nanofiltration, *Sep. Purif. Technol.*, 14 (1998) 155–162.
- [33] M.R. Teixeira, M.J. Rosa, M. Nyström, The role of membrane charge on nanofiltration performance, *J. Memb. Sci.*, 265 (2005) 160–166.
- [34] J.J. Morgan, Applications and limitations of chemical thermodynamics in water systems, In: *Equilib. Concepts Nat. Water Syst.*, American Chemical Society, Washington, 1967.
- [35] S. Bordoloi, M. Nath, R.K. Dutta, pH-conditioning for simultaneous removal of arsenic and iron ions from groundwater, *Process Saf. Environ. Prot.*, 91 (2013) 405–414.